Powerful Anticolon Tumor Effect of Targeted Gene Immunotherapy Using Folate-Modified Nanoparticle Delivery of CCL19 To Activate the Immune System

Xiaoxiao Liu,[†,§,▽] Bilan Wang,[‡,▽] Yanyan Li,[†,∥,▽] Yuzhu Hu,[†] Xiaoling Li,[†] Ting Yu,[†] Yan Ju,[†] Tao Sun,[⊥] Xiang Gao,*[†,#] and Yuquan Wei[†]

[†]Department of Neurosurgery and Institute of Neurosurgery, State Key Laboratory of Biotherapy/Collaborative Innovation Center for Biotherapy, West China Hospital, West China Medical School, Sichuan University, Chengdu, 610041, PR China

[‡]Department of Pharmacy, West China Second University Hospital of Sichuan University, Chengdu, 610041, PR China

[§]Department of Radiation Oncology, Cancer Center, Affiliated Hospital of Xuzhou Medical University; Jiangsu Center for the Collaboration and Innovation of Cancer Biotherapy, Cancer Institute, Xuzhou Medical University, Xuzhou, 221000, China

[∥]Department of Radiation Oncology, Fudan University Shanghai Cancer Center, Department of Oncology, Shanghai Medical College, Fudan University, Shanghai 200032, China

[⊥]Key Laboratory of Smart Drug Delivery of Ministry of Education, State Key Laboratory of Medical Neurobiology, Department of Pharmaceutics, School of Pharmacy, Fudan University, Shanghai 200032, PR China

[#]West China School of Basic Medical Sciences & Forensic Medicine, Sichuan University, Chengdu 610041, PR China

Ⓢ Supporting Information

ABSTRACT: Targeted gene delivery systems have recently shown potential clinical benefits in cancer treatment. Recently, the immunologic therapies application in cancer therapy also showed a continuously increase. CCL19 has shown its great potential as a candidate immunomodulator for colon cancer therapy by increasing the possibility of interaction among dendritic cells, T and B cells in secondary lymphatic tissue, thus regulating the primary (or secondary) adaptive immune responses. In this work, a folic acid modified targeted gene-delivery system consisting of DOTAP, MPEG-PLA, and Fa-PEG-PLA (F-DMA) was developed successfully through a self-assembly approach. We proved that CCL19 expression was much higher in cancer cells after transfection with F-DMA/CCL19 than after transfection with DMA/CCL19. The supernatant from cancer cells transfected with both F-DMA/CCL19 and DMA/CCL19 stimulated the activation and cytotoxicity of T lymphocytes, the maturation of DCs, and the polarization of macrophages in vitro. Moreover, the administration of F-DMA/CCL19 complex to treat tumor-bearing mice has shown significant cancer growth repression in both subcutaneous and peritoneal models. The underling antitumor mechanism is established through repressing neovascularization, promoting apoptosis, as well as reducing proliferation by activating the immune system. The CCL19 plasmid and F-DMA complex may be used as a novel method for colorectal cancer therapy in the clinic.
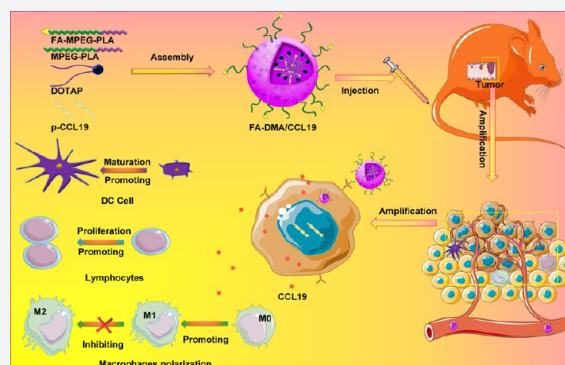
INTRODUCTION

Gene therapy is a therapeutic approach including the delivery of DNA or RNA.[1−3] However, the safety profile and the efficiency of tumor gene therapy had been restricted due to the lack of a cancer cell targeted delivery system.[4−6] Although folate is a essential ingredient for cell metabolism and DNA synthesis,[7] folate receptors (FRs) are limited expressed or almost absent in normal tissues while they are prominently expressed in tumor tissues.[8−10] It is reported that the FR is overexpressed in approximately 30−40% of human colorectal carcinoma tissues, and its expression is also associated with the proliferation, migration, and invasion of tumor cells.[11]

Therefore, FR-targeted gene therapy is a potential method to improve colon cancer treatment efficacy.

Colorectal cancer (CRC) is a primary cause of morbidity and mortality in the word.[12−15] Despite the substantial progress in treatment modalities, the prognosis and survival status of CRC patients have not improved significantly.[13] Hence, less toxic therapeutic agents are destined to improve the survival status and even quality of life which are associated with CRC.[15−17]
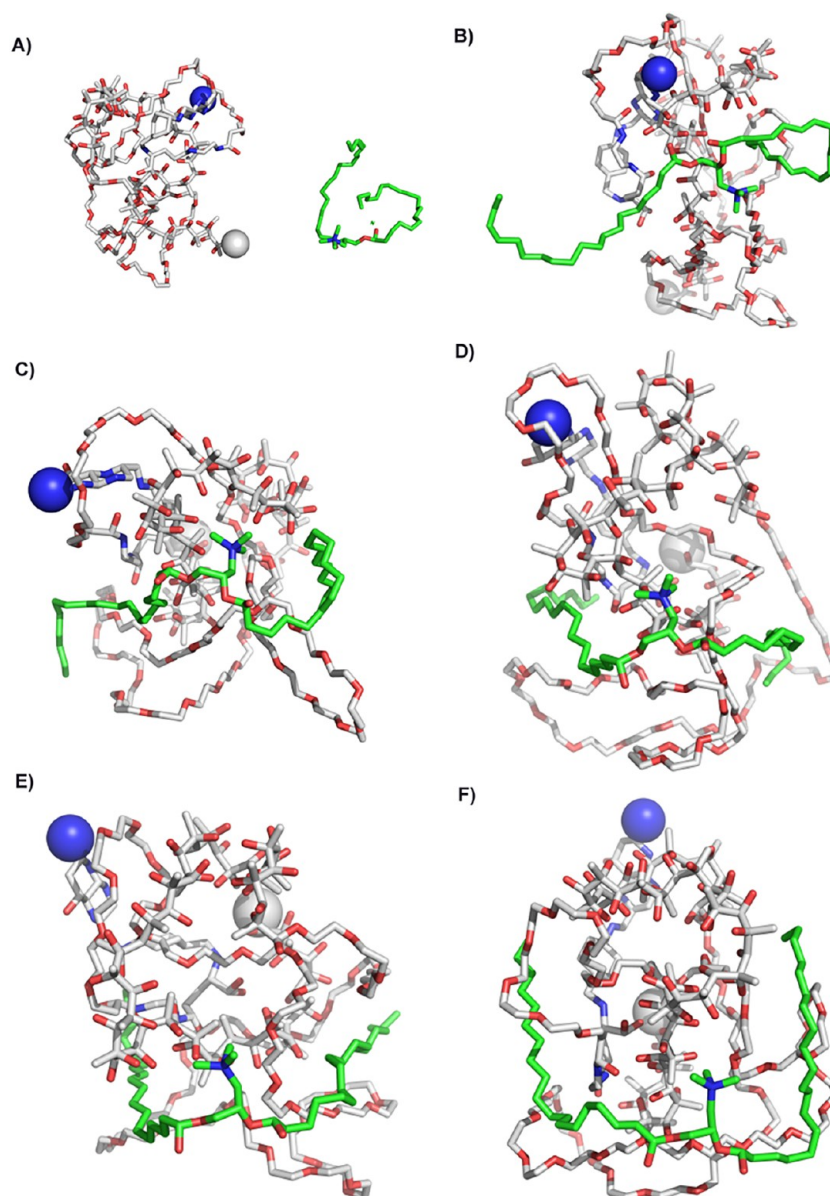
Figure 1. Interaction modes between copolymer and DOTAP revealed by Langevin dynamics simulation in water. (A) The initial conformation of FA-PEG-PLA copolymer complexed with DOTAP. Conformations (B), (C), (D), (E), and (F) correspond to snapshots of the complex collected at 100 ps, 200 ps, 300 ps, 400 and 500 ps, respectively. Copolymer FAMPEG-PLA is represented by a thin line. DOTAP is depicted by a thick line, and its carbon atoms are colored green. Two terminal heavy atoms in the FA-PEG-PLA copolymer are highlighted using a "ball" style.

Chemokine (C−C motif) ligand 19 (CCL19), a ligand of the chemokine receptor C−C chemokine receptor type 7 (CCR7), is expressed abundantly in the T-cell zones, such as lymph nodes and thymus. CCR7 chemokines and CCL19 are vital regulators of immune responses, because they regulate the migration of dendritic cells (DCs) and T cells into secondary lymphatic tissues, thus organizing the formation of immune synapse.[18−21] In addition, recent studies have suggested that DCs themselves are also able to release CCL19 during activation and migration.[22,23] Therefore, CCL19 increases the probability of interactions between dendritic cells and lymphocytes in secondary lymphatic tissue and is able to regulate the primary and/or secondary adaptive immune responses. However, the reported CCL19 gene therapy showed low efficiency and was not widely applied in CRC treatment. In our study, the CCL19 was loaded by the folate-modified particleplexes, a novel self-assembly gene delivery

system by using methoxy poly(ethylene glycol)-poly(lactide) (MPEG-PLA) and DOTAP. We proved that the transfected cancer cells could express and secrete high levels of CCL19, which will activate the immune system and show powerful antitumor responses subsequently. Additionally, the potential toxicity was dramatically decreased, and the long lasting expression of CCL19 stimulated stronger antitumor immune reactions. Moreover, the present research also studied the pharmaceutical property, in vitro biological activities, in vivo antitumor activity, antitumor mechanisms, and elementary toxicity assessment of DOTAP/FAPEG-PLA-CCL19 (F-DMA/CCL19).

■ RESULTS

Preparation and Characterization of FA-PEG-PLA and F-DMA/CCL19. FA-PEG-PLA was prepared by the method described in Supplemental Figure 1. First, HOOC-PEG-PLA
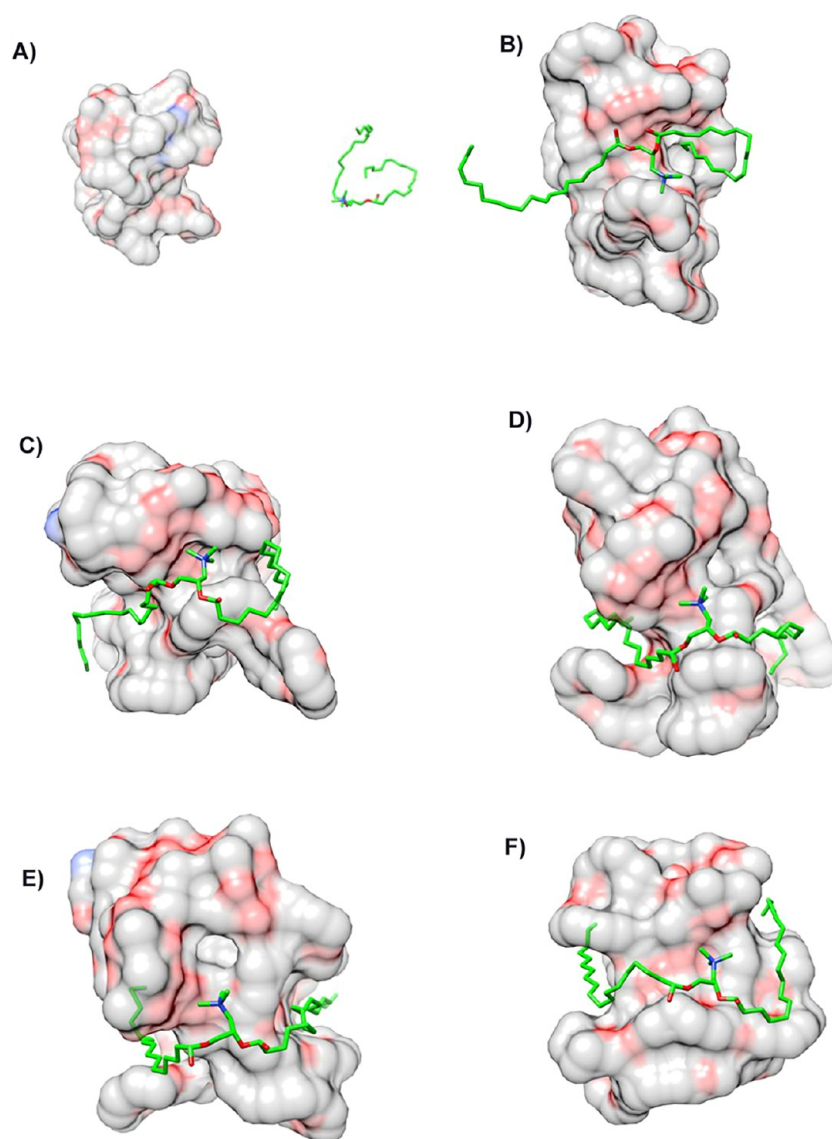
Figure 2. Interaction modes between FA-PEG-PLA copolymer and DOTAP revealed by Langevin dynamics simulation near water. (A) The initial conformation of FA-PEG-PLA copolymer complexed with DOTAP. Conformations (B), (C), (D), (E), and (F) correspond to snapshots of the complex collected at 100 ps, 200 ps, 300 ps, 400 and 500 ps, respectively. Copolymer PEG and PLA are depicted with a solid surface and colored by elements and green, respectively.

was synthesized by a classic ring-opening reaction of lactide induced by PEG-COOH catalyzed by Sn(Oct)2. Folic acid was first linked with ethylenediamine and then coupled with PEG-COOH under DCC/NHS conditions to obtain the crude product. The final targeting polymer was further purified by dialysis to give TM as a white powder. The compound was characterized by ^{1}H NMR, where the peaks were carefully distributed to the proton (Supplemental Figure 2).

F-DMA and F-DMA/CCL19 were prepared through a self-assembly process. First, the interaction between FA-PEG-PLA and DOTAP was evaluated by molecular dynamics simulation. The interaction between DOTAP and FA-PEG-PLA in aqueous solution allowed them to get close (Figure 1 and Figure 2). DOTAP adjusted its position and conformation in order to seek an interaction site on the surface of FA-PEG-PLA. Concurrently, FA-PEG-PLA changed its conformation so as to create place for DOTAP, and the interaction between them is stable. The TEM images showed that the

morphological characteristic of F-DMA and F-DMA/CCL19 (model was presented in Figure 3A) were spherical particles and had a size of approximately 47 and 53 nm, respectively (Figure 3B). The sizes of F-DMA and F-DMA/CCL19 were 92 and 108 nm (Figure 3C). The zeta potential of F-DMA/CCL19 was 7 mv (Figure 3D). DNA mobility shift assay was conducted to determine the gene-loaded capability of the F-DMA particles. The unwrapped DNA in the nanoparticles appeared as a bright band (lanes 1 to 12) (weight ratio of F-DMA/DNA: 1 to 3:0:1; 4 to 6:10:1; 7 to 9:25:1; 10 to 12:50:1), and no other bright band was observed from lanes 10 to 12 (Figure 3E). Results indicated that the CCL19 DNA was completely encapsulated in the particleplexes at a weight ratio of F-DMA/DNA of 50:1 (Figure 3E).

According to the observation under a fluorescence microscope, F-DMA had a high GFP transfection efficiency after 24 h (Figure 4A). The transfection rate was 35.1% (DMA) and 56.9% (F-DMA) detected by the flow cytometry method
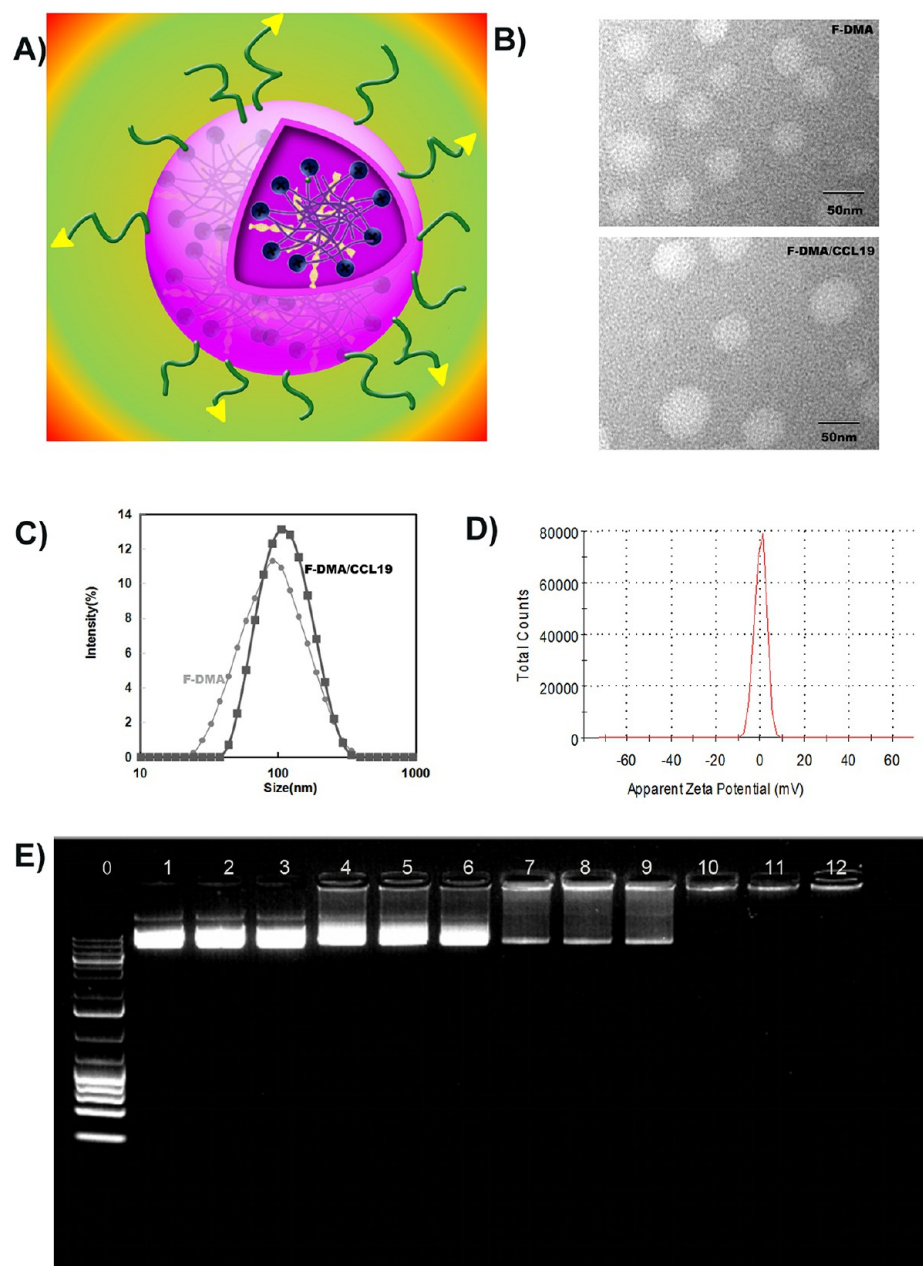
Figure 3. Physicochemical properties of F-DMA/CCL19. (A) The structure model of F-DMA/CCL19. (B) Morphological characteristics of F-DMA and F-DMA/CCL19 by TEM observation. (C) Particle sizes of F-DMA and F-DMA/CCL19. (D) Zeta-potential of F-DMA/CCL19 particleplexes. (E) Gel retardation assay of DNA and particleplexes. Lane 0, DNA marker; lane 1−3, naked CCL19; lanes 4−12, different weight ratios of CCL19 with F-DMA. CCL19 was completely incorporated into F-DMA at a weight ratio of 1:50 in lanes 10−12, and particleplexes were prepared without free DNA.

(Figure 4B). The supernatant of CT26 cells incubated with GS, F-DMA, F-DMA/pVax, DMA/CCL19, or F-DMA/CCL19 was analyzed for CCL19 expression. A higher concentration of CCL19 was found in the F-DMA/CCL19 group than that in other groups (Figure 4C).

F-DMA/CCL19 Stimulated the Activation of T Lymphocytes, Maturation of DCs and Polarization of Macrophages. Herein, we speculated that the antitumor ability of CCL19 was attributed to the activation of DC and T cell. Transfection of CT26 cells with GS, F-DMA, F-DMA/pVax, DMA/CCL19, or F-DMA/CCL19 for 72 h was conducted, of which the supernatant was collected for lymphocyte, DC and macrophage culture for 24 h. We

analyzed the subset of lymphocytes and found that the amounts of $CD_4^+CD_{69}^+$ and $CD_8^+CD_{69}^+$ lymphocytes in the DMA/CCL19 or F-DMA/CCL19 were more than those in other treatment groups (GS, F-DMA, F-DMA/pVax) (Figure 5A,B). F-DMA/CCL19 or DMA/CCL19 treatment improved the level of $CD_4^+IFN-\gamma^+$ and $CD_8^+IFN-\gamma^+$ T cells compared to other treatments (Figure 5C,D).

The numbers of MHC-II$^+$ and CD86$^+$ DCs also increased to 42.96% and 40.81% of the F-DMA/CCL19 group compared to the corresponding 29.25% and 28.33% in the GS control group (Figure 6).

In addition, the F-DMA-CCL19 treatment reduced the polarization of the macrophage to the M2 phenotype (Figure
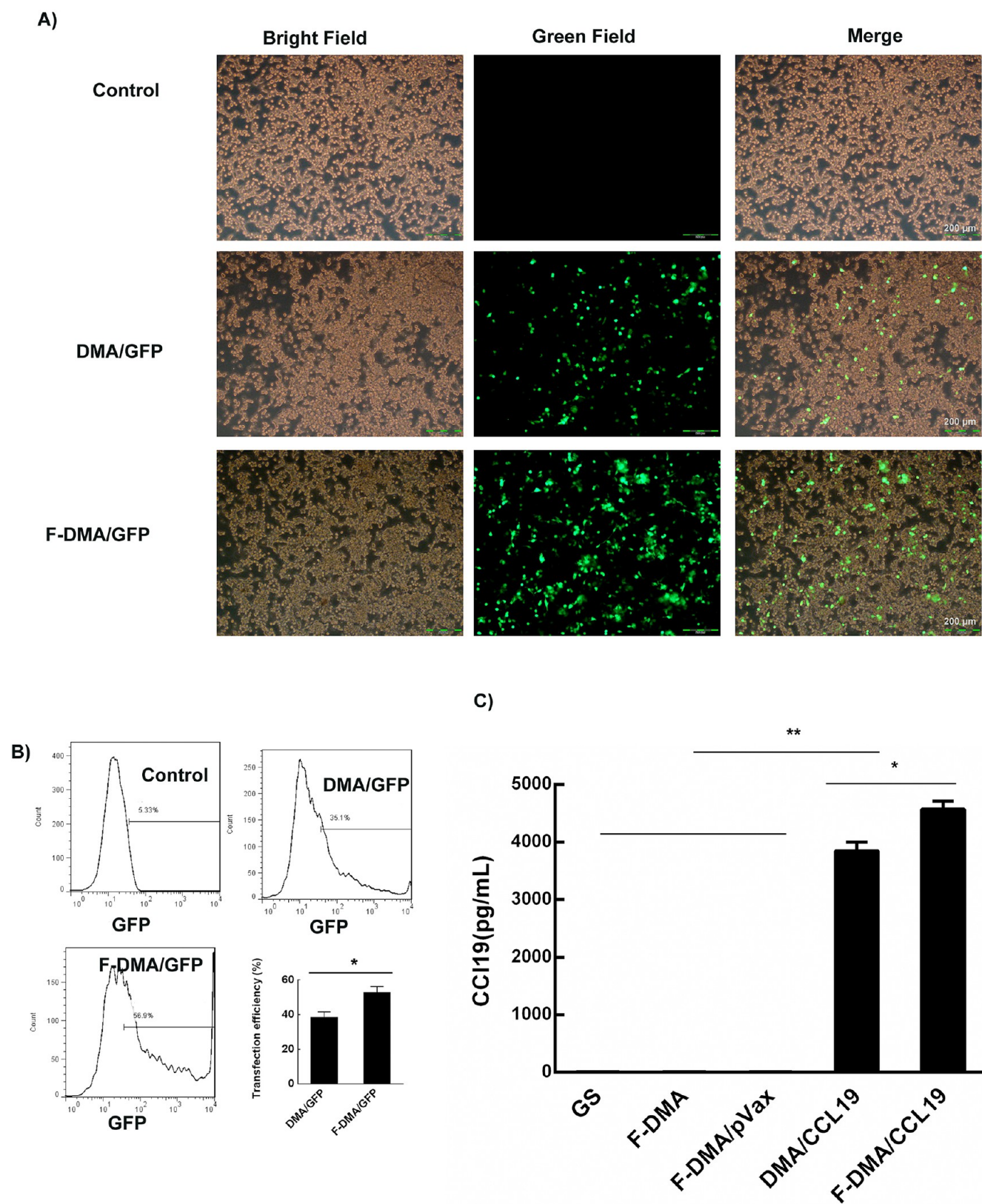
Figure 4. Transfection efficiency test of F-DMA/CCL19. DMA/F-DMA containing pEGFP (4 μg) was used to transfect CT26 cells at a weight ratio of 1:50 pEGFP to DMA and F-DMA. The transfection efficiency was measured by fluorescence microscopy (A) and flow cytometry after 24 h (mean ± SEM, $n = 3$; * $p < 0.05$, **$p < 0.01$; F-DMA/GFP versus DMA/GFP) (B). Detection of CCL19 in cell supernatant from different groups by ELISA (mean ± SEM, $n = 3$; *, $p < 0.05$, **, $p < 0.01$; F-DMA/CCL19 versus DMA/CCL19; F-DMA/CCL19, DMA/CCL19 versus GS, DMA, DMA/pVax) (C). Scale bar is 200 μm. The results represent three independent experiments.
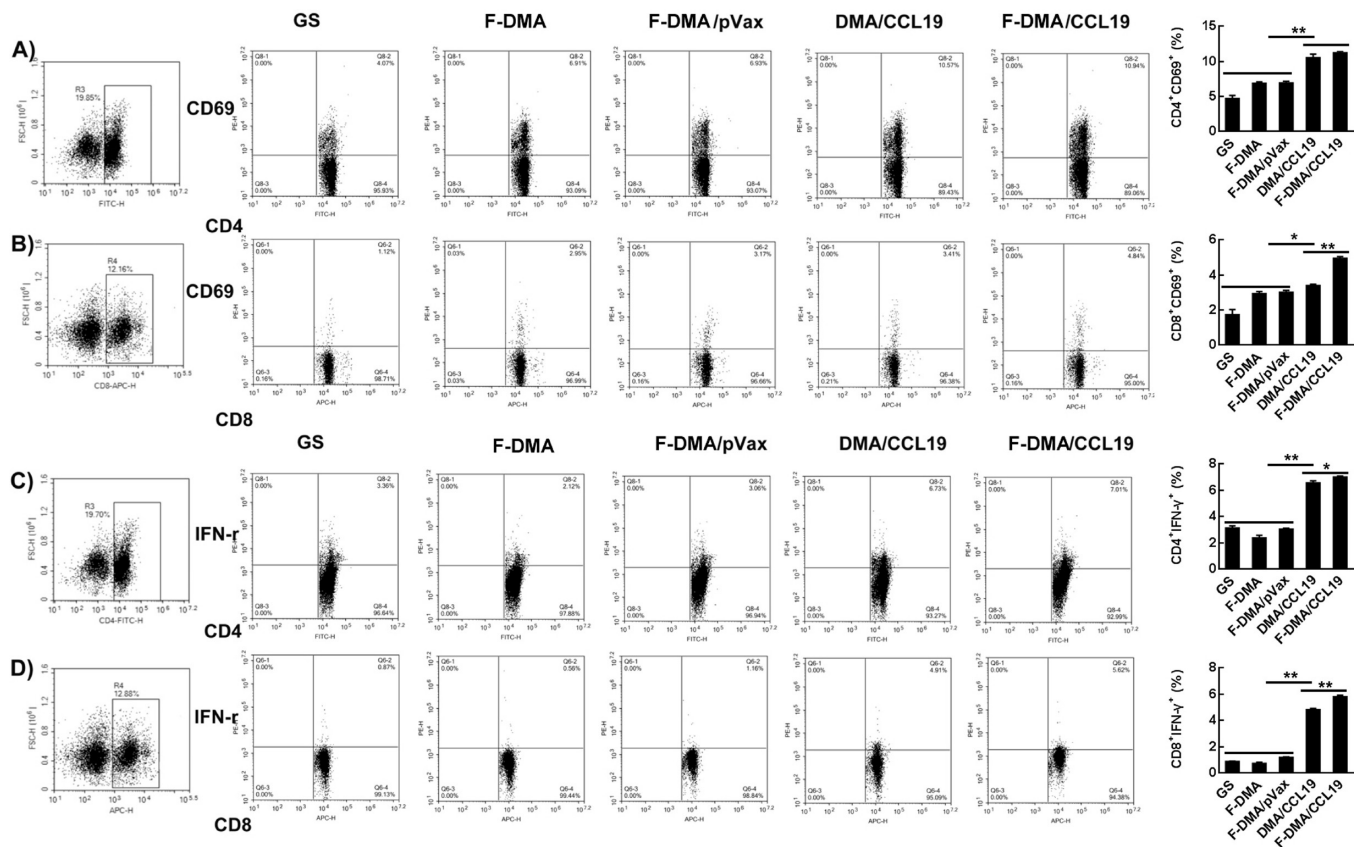
Figure 5. Treatment with F-DMA/CCL19 activated T cells in vitro. When CT26 cells were transfected with GS, F-DMA, F-DMA/pVax, DMA/CCL19, and F-DMA/CCL19 for 72 h, the supernatants from different treatments were added to spleen-derived lymphocytes and treated for 24 h. The subsets of CD4$^+$CD69$^+$ (A), CD8$^+$CD69$^+$ (B), CD4$^+$IFN-γ^+ (C), and CD8$^+$IFN-γ^+ (D) lymphocytes were tested by flow cytometry. (mean $\pm$ SEM, n = 3; *, $p < 0.05$, **, $p < 0.01$; F-DMA/CCL19 versus DMA/CCL19; F-DMA/CCL19, DMA/CCL19 versus GS, DMA, DMA/pVax) The results represent three independent experiments.

Figure 6. Treatment with F-DMA/CCL19-induced maturation of DCs. When CT26 cells were transfected with GS, F-DMA, F-DMA/pVax, DMA/CCL19, and F-DMA/CCL19 for 72 h, the supernatants from different treatments were added to DCs and treated for 24 h. The subsets of MHC-II$^+$ (A) and CD86$^+$ (B) DCs were tested by flow cytometry (mean $\pm$ SEM, n = 3; *, $p < 0.05$, **, $p < 0.01$; F-DMA/CCL19 versus DMA/CCL19; F-DMA/CCL19, DMA/CCL19 versus GS, DMA, DMA/pVax). The results represent three independent experiments.
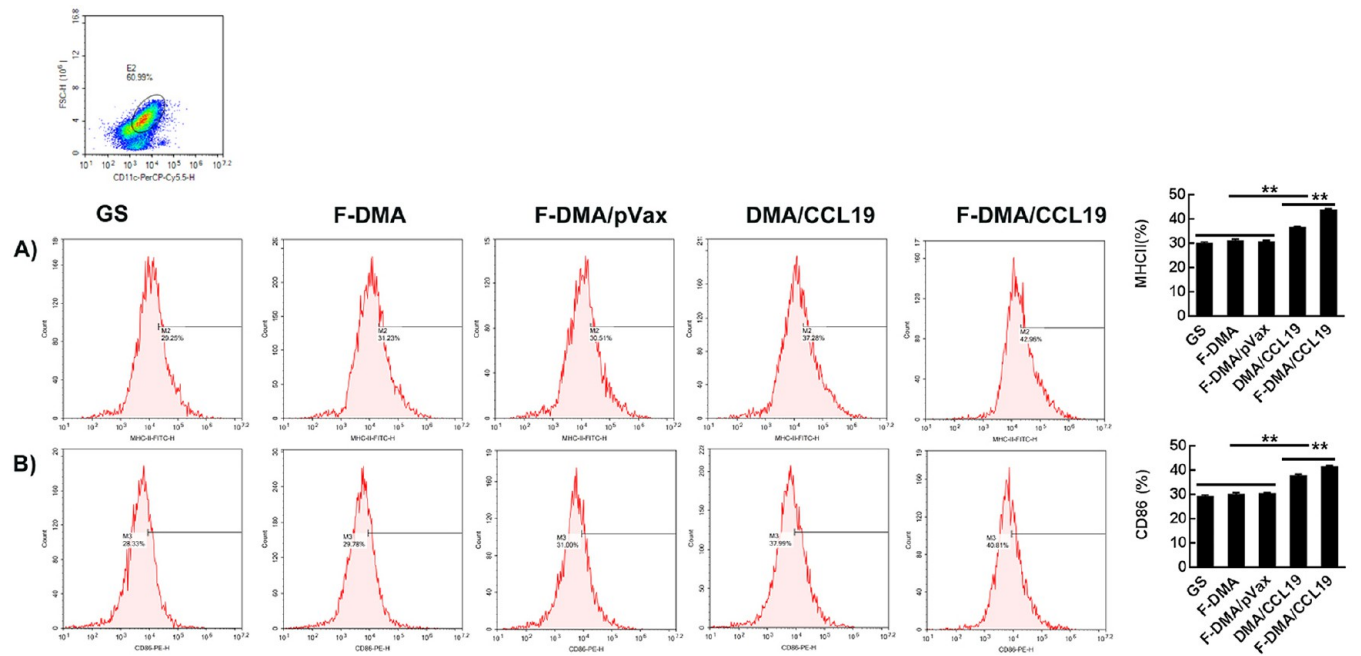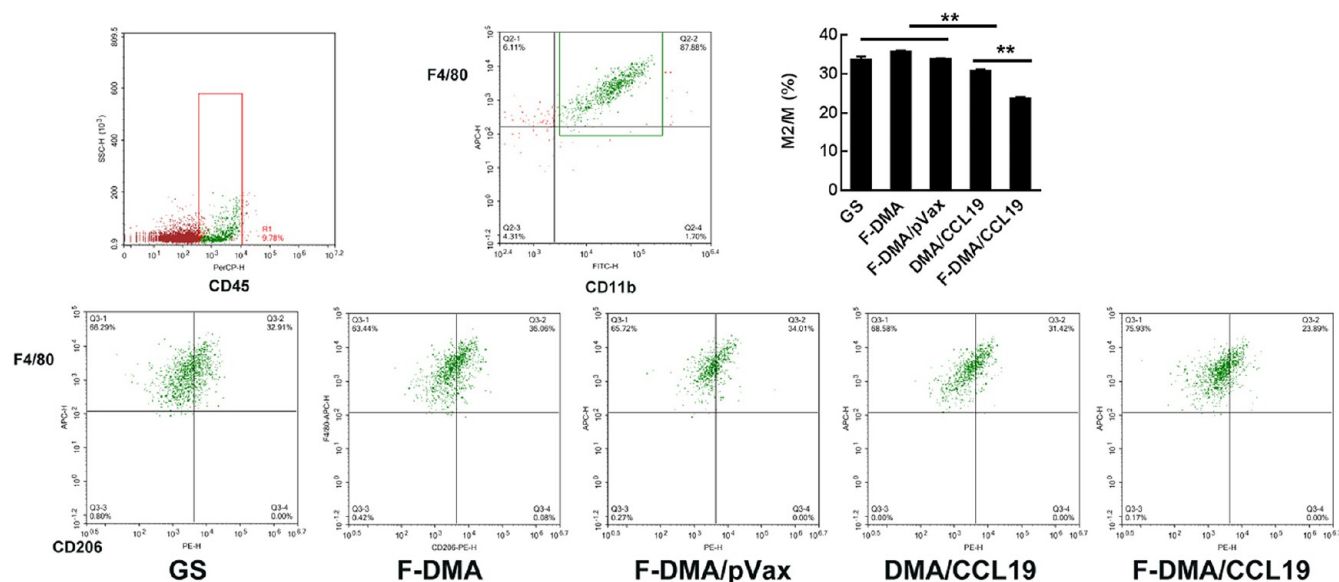
Figure 7. Treatment with F-DMA/CCL19 programmed macrophage phenotype to M1. When CT26 cells were transfected with GS, F-DMA, F-DMA/pVax, DMA/CCL19, and F-DMA/CCL19 for 72 h, the supernatants from different treatments were added to peritoneal derived macrophage cells and treated for 24 h. The cells were stained with CD45, CD11b, F4/80, and CD206 antibodies. The percentage of $CD11b^+F4/80^+CD206^{high}$ M2 macrophage cells is shown (mean $\pm$ SEM, $n = 3$; *, $p < 0.05$, **, $p < 0.01$; F-DMA/CCL19 versus DMA/CCL19; F-DMA/CCL19, DMA/CCL19 versus GS, DMA, DMA/pVax). The results represent three independent experiments.

7). Specifically, the $CD45^+CD11b^+F4/80^+CD206^{high}$ cells of the control group were 33%, while the F-DMA/CCL19 treatment decreased the rate to 23% (Figure 7).

Most importantly, F-DMA/CCL19 treatment triggered a higher number of $CD_4^+CD_{69}^+$, $CD_8^+CD_{69}^+$, $CD_4^+IFN\text{-}\gamma^+$, and $CD_8^+IFN\text{-}\gamma^+$ T lymphocytes and elevated $MHC\text{-}II^+$, $CD86^+DC$, and $CD11b^+F4/80^+CD206^{low}$ M1 phenotype to a greater degree than the DMA/CCL19 group.

F-DMA/CCL19 Increased the Cytotoxic Effect of Lymphocytes. The supernatant from CT26 cells transfected with GS, F-DMA, F-DMA/pVax, DMA/CCL19, or F-DMA/CCL19 for 72 h was used for lymphocyte incubation for 24 h. It was observed that the lymphocyte proliferation (Figure 8A) was significantly more in the F-DMA/CCL19 group than in control groups. Moreover, EdU was used to mark the lymphocytes in order to further identify which subset proliferated, and the results showed that the proliferated lymphocytes were CD8+ cells (Supplemental Figure 3).

The supernatant of lymphocyte treated after 24 h was then used as the culture medium for CT26 cells. In our experiments, the proliferative response of CT26 cells was reduced by F-DMA/CCL19 treatment in comparison with GS, F-DMA/pVax or DMA/CCL19 treatment ($P < 0.05$). The mock vector (F-DMA) alone did not induce a cytotoxic response (Figure 8B).

We observed that the secretion of TNF-α and IFN-γ were significantly increased in the F-DMA/CCL19 group than in other groups (Figure 8C,D). In addition, macrophages cultured with the supernatant derived from the F-DMA/CCL19-transfected CT26 cells also secreted higher levels of TNF-α and IFN-γ than the control group (Figure 8E,F).

In Vivo Antitumor Effect of F-DMA/CCL19. In vivo bioluminescence imaging also showed higher gene delivery efficiency to tumor tissue in mice given F-DMA/pDNA treatment than that given DMA/pDNA treatment (Figure 9). And there is no difference in organs between F-DMA/pDNA and DMA/pDNA group (Supplemental Figure 4A). And the

expressions of CCL19 of different groups in the same normal tissue are uniform (Supplemental Figure 4B).

DMA/F-DMA and its corresponding particleplexes loaded with CCL19 were given to BALB/c mice with CT26 colon cancer by tail intravenous injection. There was an obvious retardation of tumor growth induced by therapy with F-DMA/CCL19 and DMA/CCL19, whereas mice injected with GS, F-DMA, or F-DMA/pVax showed a rapid increase in the tumor size. Both F-DMA/CCL19 and DMA/CCL19 treatments showed good antitumor effect relative to other particleplexes (F-DMA/pVax and GS), while no obvious differences were found among other treatment groups. In addition, F-DMA/CCL19 showed a better antitumor effect than DMA/CCL19 (Figure 10). No significant difference of body weight was found among all the treatment groups (Figure 10).

Moreover, similar antitumor phenomenon was observed in the CT26 peritoneal model. The tumor nodules of mice administrated with F-DMA/CCL19 were fewer and smaller than other groups. Additionally, F-DMA/CCL19 administration also reduced the ascite fluid compared with other treatments (Figure 11).

F-DMA/CCL19 Administration Resulted in Enhanced Immune Responses. We collected the peritoneal fluid, serum, and tumor nodules for analysis, and F-DMA/CCL19 administration increased the expression of CCL19, TNF-α, and IFN-γ in all experimental samples compared with the control groups (Figure 12).

To evaluate how F-DMA/CCL19 administration affected immune reactions, spleen tissues were subjected for flow cytometry to analyze the composition of different immune effector cells. F-DMA/CCL19 treatment activated T lymphocytes, as shown by the increased level of CD69+CD4+ (Supplemental Figure 5A) and $CD69^+CD8^+T$ (Supplemental Figure 5B) cells. In addition, mice treated with F-DMA/CCL19 had more $CD4^+IFN\text{-}\gamma^+$ (Supplemental Figure 5C) and $CD8^+IFN\text{-}\gamma^+$ (Supplemental Figure 5D) T cells, demonstrating that the antitumor effect could also be attributed to an increase
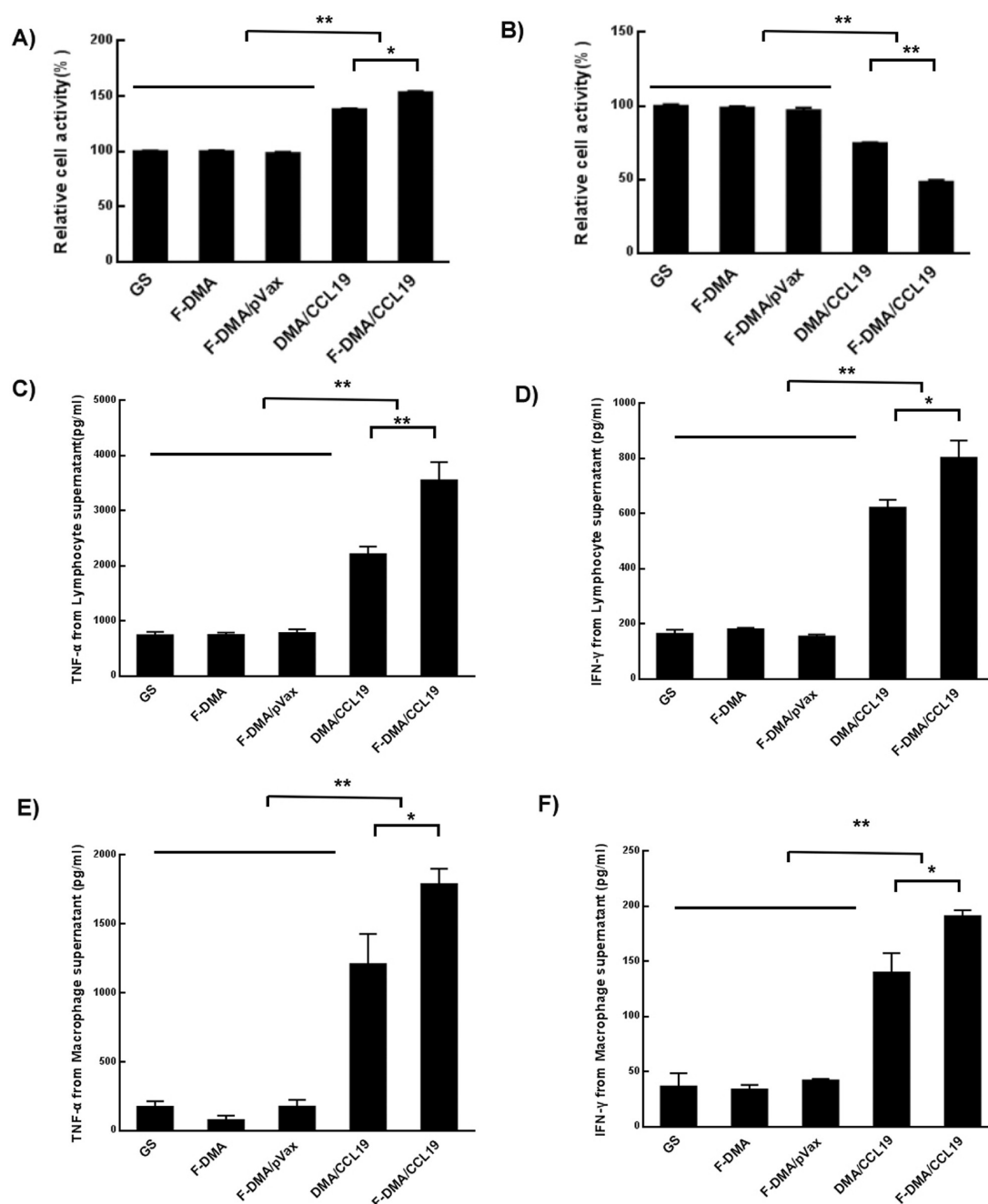
Figure 8. F-DMA/CCL19 stimulated the cytotoxicity of T lymphocytes. When CT26 cells were transfected with GS, F-DMA, F-DMA/pVax, DMA-CCL19, and F-DMA/CCL19 for 72 h, the supernatants from different treatments were added into lymphocytes and treated for 24 h, and the lymphocyte activity was tested by the MTT test (A). When the lymphocytes were treated for 24 h, the supernatants were added to CT26 cells and treated for 24 h, and the CT26 cell activity was tested by MTT (B). The lymphocytes were treated for 24 h with cell culture supernatants collected from GS. F-DMA, F-DMA/pVax, DMA/CCL19, and F-DMA/CCL19 groups, and the corresponding supernatants after 24 h of culture in each group were then collected for measurement of IFN-γ (C) and TNF-α (D) level. The lymphocytes were treated for 24 h with cell culture supernatants collected from GS, F-DMA, F-DMA/pVax, DMA/CCL19, and F-DMA/CCL19 groups, and the corresponding supernatants were then applied to culture macrophages, and then the culture medium was collected for measurement of IFN-γ (E) and TNF-α (F). F-DMA/CCL19 mediated IFN-γ and TNF-α expression was substantially higher than that of other groups. *$p < 0.05$, **$p < 0.01$ when compared with GS, F-DMA, or F-DMA/pVax-treated groups. The results represent three independent experiments.

of cytotoxic T lymphocytes (CTL). Moreover, F-DMA/CCL19 administration also significantly decreased the amounts of Tregs (Supplemental Figure 5E).

F-DMA/CCL19 administration also polarized macrophages to the M2 phenotype. The percentages of CD45^{+}CD11b^{+}F4/80^{+}CD206^{high} macrophage cells in the peritoneal fluid (Supplemental Figure 6A)) and tumor (Supplemental Figure 6B)) were remarkably reduced after F-DMA/CCL19 treatment in the peritoneum colon cancer model compared with other groups. We also found the MDSCs (Gr1^{+}CD11b^{+}) in spleens and peritoneal cells percentages were significantly decreased after F-DMA/CCL19 treatment compared with control treatments (Supplemental Figure 7).
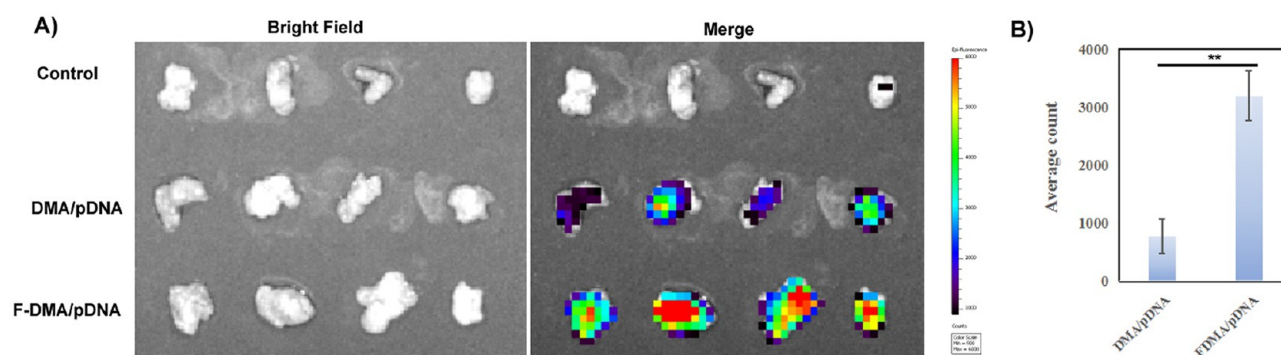
Figure 9. Imaging in vivo. First, pDNA was labeled with toto-3, and then the gene was carried by DMA and F-DMA. Mouse with abdominal tumor was administered with DMA/pDNA and F-DMA/pDNA labeled with toto-3 through intraperitoneal injection. (A) Images were taken by the IVIS Lumina imaging system after 5 h. (B) The content of pDNA in tumors in different groups (mean ± SEM, $n = 4$; **$p < 0.01$; F-DMA/pDNA versus DMA/pDNA), The results represent three independent experiments.
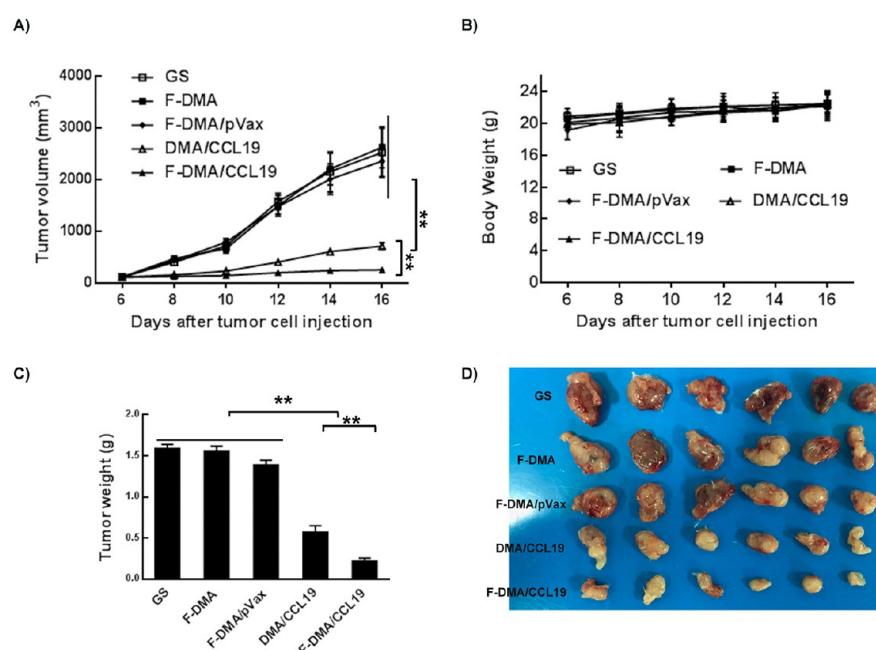

Figure 10. Anticolon cancer effect of F-DMA/CCL19 in subcutaneous tumor model. (A) Tumor growth curves. (B) Body weight of different groups. (C) Tumor weight. (D) Tumor photos of GS, F-DMA, F-DMA/pVax, DMA-CCL19, and F-DMA/CCL19 treatment groups. Mean ± SEM, $n = 6$; *$p < 0.05$, **$p < 0.01$ when compared with GS-treated group. The results represent three independent experiments.

F-DMA/CCL19 Induced Immune Cell Infiltration and Cancer Cell Apoptosis, Inhibited Tumor Cell Proliferation and Suppressed Tumor Angiogenesis. As well-known, CD8^{+} lymphocytes and macrophages are main antitumor effector cells. Therefore, CD8 and F4/80 were used to test lymphocytes and macrophages. We found that CD8 lymphocytes and macrophages infiltrated into tumor tissue after F-DMA/CCl19 and DMA/CCl19 treatment. And the amounts were much higher in F-DMA/CCl19 treatment group than those in the DMA/CCL19 (Supplemental Figure 8).

Ki67 staining of tumor sections from different treatment groups was performed to evaluate tumor cell proliferation. Similarly, Supplemental Figure 9 showed fewer proliferating cells in the F-DMA/CCL19 group than those in other control groups. In addition, CD31 staining revealed that F-DMA/CCL19 and DMA/CCL19 groups also had a significant antiangiogenesis effect in tumors compared with other groups. Furthermore, TUNEL staining was also performed to examine tumor cell apoptosis (Supplemental Figure 9). The F-DMA/CCL19 treatment induced much more TUNEL-positive cells than those of other groups. Overall, this evidence demonstrated that F-DMA/CCL19 could successfully generate antitumor effects through inducing cellular apoptosis and suppressing tumor cell proliferation and vascular formation.

◼ SAFETY ASSESSMENT

Vital organs (heart, liver, spleen, lung, and kidney) of different treatment group mice were collected and observed by HE staining to evaluate the safety of particleplexes. Results showed normal histological morphology in all the treatment groups, and no toxicity of F-DMA/CCL19 was found (Supplemental Figure 8). Besides, hematological index analysis showed no obvious toxicities (Supplemental Figures 10–12).
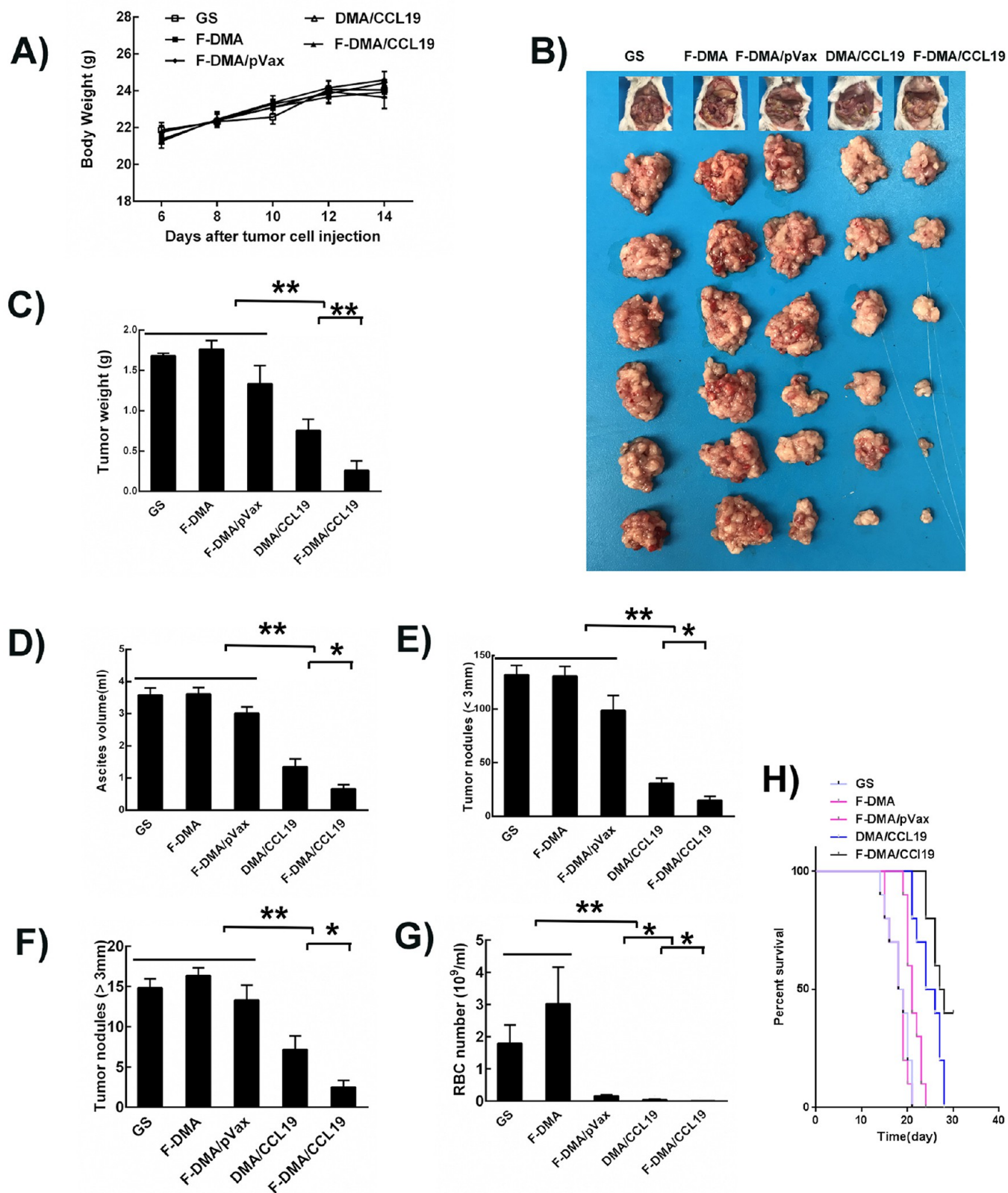
Figure 11. Anticolon cancer effect of F-DMA/CCL19 in peritoneal colon cancer model. (A) Body weight. (B) Images of mouse and the corresponding tumor. (C) Tumor weight of different group (GS, F-DMA, F-DMA/pVax, DMA/CCL19, and F-DMA/CCL19-treated mice). (D) Ascites volumes of different groups. The number of tumor nodes in different groups: (E) Tumor nude (<3 mm) of different groups; (F) Tumor nude (>3 mm) of different groups. (G) Red blood cell number in ascites of different groups. (H) Survival curve detection of different groups. Mean ± SEM, $n = 6$; $*p < 0.05$, $**p < 0.01$ when compared with GS-treated group. The results represent three independent experiments.

Figure 12. F-DMA/CCL19 increased CCL19, IFN-γ and TNF-α expression in peritoneal colon cancer model. Peritoneal fluid, tumor tissue and serum of the five groups (GS, F-DMA, F-DMA/pVax, DMA/CCL19, and F-DMA/CCL19) were collected after two doses, and we measured the expression of CCL19, IFN-γ and TNF-α by ELISA in the peritoneal fluid (A), tumor tissue protein (B), and serum (C). Mean $\pm$ SEM, $n = 5$; *$p <$ 0.05, **$p < 0.01$ when compared with GS-treated group. The results represent three independent experiments.

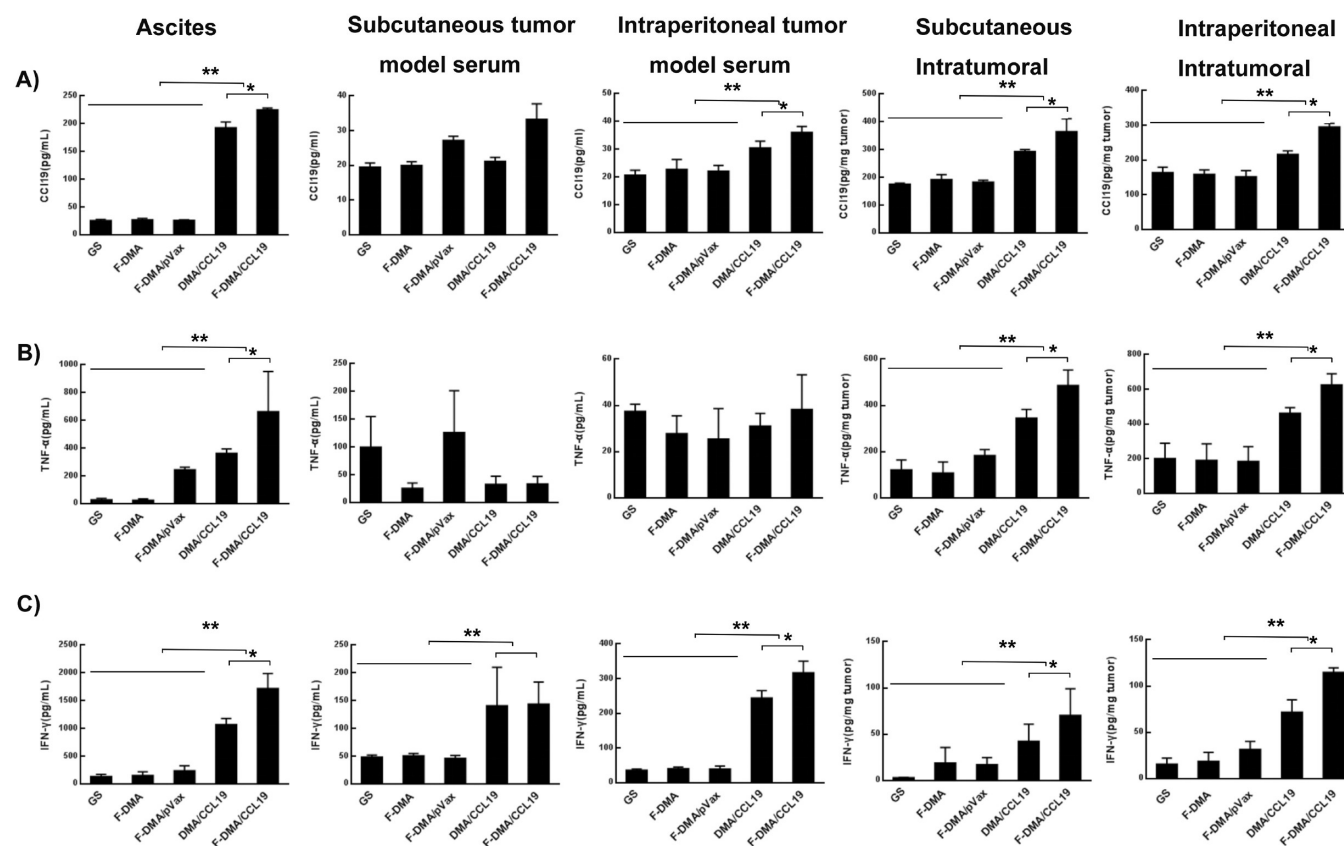## ■ DISCUSSION

In this research, we certified that the F-DMA based particleplexes obviously improved the transfection efficiency of CCL19 in CT26 cells as detected in vivo photography. The treatment of F-DMA/CCL19 to tumor-bearing mice exhibited significantly inhibition of tumor growth and reduced the burden of ascite formation. When compared to DMA/CCL19 and other groups, the F-DMA/CCL19 group showed a substantially increased expression of CCL19 in tumor tissues of mice, which might be beneficial from the F-DMA carriers. As detected in tumor sections, the potential antitumor effect was also realized by inducing apoptosis of tumor cells, suppressing proliferation and angiogenesis of tumors. Most importantly, F-DMA/CCL19 administration mainly stimulates the immune system, which is supported by our study results. Namely, a significant decrease in the percentages of MDSCs and CD4+Foxp3+ Tregs after F-DMA/CCL19 treatment showed by the flow cytometry assay. In the meantime, the percentages of CD8$^+$ T cells, CD8$^+$CD69$^+$ T cells, CD4$^+$IFN-γ^+ T cells, and CD8$^+$IFN-γ^+ T cells were increased. Furthermore, we assessed the elementary safety of F-DMA/CCL19, and obseved no abnormalities in the vital organs of all groups of mice. So, we deduce that the F-DMA gene delivery system is a potential anticancer agent with a better safety profile, which enhanced the effectiveness of gene expression and targeted therapy.

Cancer gene therapy, a therapeutic delivery of RNA or DNA into the site of tumors, has caused wide attention.[24] Cancer

cells replicated highly dependent on folate. They also expressed their own receptors which are not overexpressed on normal tissue. So we can use the folate receptor for targeted anticancer treatment.[25,26] The gene delivery system contributes to improve the specific delivery and expression of therapeutic genes in tumor tissue, thereby increasing the gene therapy efficacy. Another purpose of this work was to form a new folate modified carrier, attempting to overcome the low transfection efficiency of the nontarget systems.

Overall, in this context, we proved that F-DMA/CCL19 gene therapy enhanced both tumor cell apoptosis and immune response induction, leading to a significant suppression in cancer growth in both subcutaneous and peritoneum colon cancer mice models. Due to tumor rejection, cellular and humoral antigen-specific immune responses were enhanced in CCL19-treated mice. In our experiment, we observed a significantly increased expression of TNF-α and IFN-γ at the tumor site, as well as in cultured lymphocytes and macrophages after the treatment of F-DMA/CCL19. IFN-γ and TNF-α are multifunctional antitumor cytokine that play an important role in cell apoptosis, inflammation, and immunity.[27−30] These cytokines may explain the high level tumor cell apoptosis, suppression of tumor cell proliferation and neovascularization in the F-DMA/CCL19-treated tumor tissue in this research. We also provided more evidence that the local cytokine environment was changed by inducing IFN-γ and TNF-α expression after CCL19 gene delivery directly into tumors, and these cytokine changes were one of the reasons of tumor regression.

F- DMA/CCL19 treatment increased the CD4$^+$CD69$^+$ and CD8$^+$CD69$^+$ population compared with the control treatment. In the F-DMA/CCL19 treated group, the production of IFN-γ by CD8$^+$ and CD4$^+$ T cells was also obviously increased, while the number of Tregs was decreased in comparison with the controls. One possible reason is that F-DMA/CCL19 treatment increased the expression of MHC-II and CD86 on DCs, which means the activation of DCs. Several studies reported CCL19 recruits DCs to treat tumor.[31−33] DCs are the most powerful antigen-presenting cells which could mediate antitumor immunity by activating T-cell responses. The recruitment of DCs was also one of the most common methods in antitumor.[34−37] Our study shows that the antitumor efficacy may be relevant with DCs recruited by CCL19 in the tumor site. Another possible reason might be that F-DMA/CCL19 treatment can lead to reduced MDSCs since MDSCs suppress the responses of T cells. A number of studies have proved that MDSCs elimination could break through immunosuppression inducing by cancer and enhance immunotherapy.[38,39] In addition, F-DMA/CCL19 treatment also reduced the macrophage polarization to the M2 phenotype. Previous studies have proved that M2-like TAMs favor tumor growth and angiogenesis, suppress adaptive immunity and promote tumors, and modulating the M1/M2 polarization status is of great importance for the development of novel therapies.[40−42] In conclusion, F-DMA/CCL19 treatment could considerably improve the antitumor immune response.

Traditional chemotherapy for tumor therapy is featured by high toxicity, poor targeting, and will always impair the immune system due to adverse effects, while the particleplexes led to an efficient antitumor activity mediated by the activation of the immune system, and it is proved safe and nontoxic in our study. Besides, targeted therapy in this work has advantage over chimeric antigen receptor T-Cell (CAR-T) technology which also effects the immune system. A recent study[43] also suggested that suitable combinations CAR with IL-7 and CCL19, mimicked the function of T-zone reticular cells and recruited T lymphocytes and dendritic cells to tumor sites. This method improved CAR-T cells antitumor activities in solid tumor. However, as CAR-T cells could lead to T-cell expansion in vivo and release of cytokines, other immune cells such as macrophages might also secrete cytokines in response to the cytokines released by the infused CAR T cells. Thus, the most common weakness of CAR-T, which restricts its wide development and application, is the release of toxic levels of cytokines, referred to as cytokine release syndrome (CRS). In contrast, our study showed F-DMA/CCL19 treatment considerably improved the antitumor immune response partly by increased cytotoxic cytokines, while these cytokines will decrease with the condition of reduced tumor burden.

In conclusion, a novel and safe F-DMA-based particleplex loaded with CCL19 (F-DMA/CCL19) was prepared successfully. Folic acid modified nanoparticles increased the uptake of CCL19 by CT26. In vitro F-DMA/CCL19 transfected CT26 cells expressed high levels of CCL19. Particleplexes led to an efficient antitumor activity mediated by activating the immune system. Therefore, F-DMA-based particleplexes with therapeutic CCL19 gene is a prospective candidate in clinical application for CRC therapy.

■ ASSOCIATED CONTENT

ⓢ Supporting Information

The Supporting Information is available free of charge on the ACS Publications website at DOI: 10.1021/acscentsci.8b00688.

Additional experimental details and figures including synthetic identification, transfection, cell culture, immune cell activation, imaging in vivo, and safety evaluation (PDF)

■ AUTHOR INFORMATION

Corresponding Author
*Tel +86 28 8542 2136. Fax +86 28 8550 2796. E-mail: xianggao@scu.edu.cn.

ORCID ⦿
Xiang Gao: 0000-0001-7478-5072

Author Contributions
▽X. Liu, B.W., and Y.L. are considered equal first authors.

Notes
The authors declare no competing financial interest.

■ REFERENCES

(1) Chen, J.; Gao, P.; Yuan, S.; Li, R.; Ni, A.; Chu, L.; Ding, L.; Sun, Y.; Liu, X. Y.; Duan, Y. Oncolytic Adenovirus Complexes Coated with Lipids and Calcium Phosphate for Cancer Gene Therapy. *ACS Nano* **2016**, *10* (12), 11548−11560.

(2) Elbakry, A.; Zaky, A.; Liebl, R.; Rachel, R.; Goepferich, A.; Breunig, M. Layer-by-layer assembled gold nanoparticles for siRNA delivery. *Nano Lett.* **2009**, *9* (5), 2059−2064.

(3) Naldini, L. Gene therapy returns to centre stage. *Nature* **2015**, *526* (7573), 351−360.

(4) Karjoo, Z.; Chen, X.; Hatefi, A. Progress and Problems with the Use of Suicide Genes for Targeted Cancer Therapy. *Adv. Drug Delivery Rev.* **2016**, *99* (Pt A), 113−128.

(5) Yang, G.; Wang, J.; Wang, Y.; Li, L.; Guo, X.; Zhou, S. An implantable active-targeting micelle-in-nanofiber device for efficient and safe cancer therapy. *ACS Nano* **2015**, *9* (2), 1161−1174.

(6) Chen, Y.; Gao, D. Y.; Huang, L. In vivo delivery of miRNAs for cancer therapy: challenges and strategies. *Adv. Drug Delivery Rev.* **2015**, *81*, 128−141.

(7) Nikkanen, J.; Forsström, S.; Euro, L.; Paetau, I.; Kohnz, R. A.; Wang, L.; Chilov, D.; Viinamäki, J.; Roivainen, A.; Marjamäki, P. Mitochondrial DNA Replication Defects Disturb Cellular dNTP Pools and Remodel One-Carbon Metabolism. *Cell Metab.* **2016**, *23* (4), 635−648.

(8) El-Gogary, R. I.; Rubio, N.; Wang, J. T.; Al-Jamal, W. T.; Bourgognon, M.; Kafa, H.; Naeem, M.; Klippstein, R.; Abbate, V.; Leroux, F.; et al. Polyethylene Glycol Conjugated Polymeric Nanocapsules for Targeted Delivery of Quercetin to Folate-Expressing Cancer Cells In Vitro and In Vivo. *ACS Nano* **2014**, *8* (2), 1384−1401.

(9) Peer, D.; Karp, J. M.; Hong, S.; Farokhzad, O. C.; Margalit, R.; Langer, R. Nanocarriers as an emerging platform for cancer therapy. *Nat. Nanotechnol.* **2007**, *2* (12), 751−760.

(10) Brannonpeppas, L.; Blanchette, J. O. Nanoparticle and targeted systems for cancer therapy. *Adv. Drug Delivery Rev.* **2004**, *56* (11), 1649−1659.

(11) van Dam, G. M.; Themelis, G.; Crane, L. M.; Harlaar, N. J.; Pleijhuis, R. G.; Kelder, W.; Sarantopoulos, A.; de Jong, J. S.; Arts, H. J.; Ag, V. D. Z.; et al. Intraoperative tumor-specific fluorescence imaging in ovarian cancer by folate receptor-α targeting: first in-human results. *Nat. Med.* **2011**, *17* (10), 1315−1319.

(12) Siegel, R. L.; Miller, K. D.; Jemal, A. Cancer statistics, 2018. *Ca-Cancer J. Clin.* **2018**, *68* (1), 7−30.

(13) Hubbard, J. M.; Grothey, A. When less is more: maintenance therapy in colorectal cancer. *Lancet* **2015**, *385* (9980), 1808−1810.

(14) Liu, Y.; Zhang, X.; Han, C.; Wan, G.; Huang, X.; Ivan, C.; Jiang, D.; Rodriguezaguayo, C.; Lopezberestein, G.; Rao, P. H.; et al. TP53 loss creates therapeutic vulnerability in colorectal cancer. *Nature* **2015**, *520* (7549), 697−701.

(15) Naxerova, K.; Reiter, J. G.; Brachtel, E.; Lennerz, J. K.; van de Wetering, M.; Rowan, A.; Cai, T.; Clevers, H.; Swanton, C.; Nowak, M. A.; Elledge, S. J.; Jain, R. K. Origins of lymphatic and distant metastases in human colorectal cancer. *Science* **2017**, *357* (6346), 55−60.

(16) Kreso, A.; van Galen, G. P.; Pedley, N. M.; Lima-Fernandes, E.; Frelin, C.; Davis, T.; Cao, L.; Baiazitov, R.; Du, W.; Sydorenko, N.; et al. Self-renewal as a therapeutic target in human colorectal cancer. *Nat. Med.* **2014**, *20* (1), 29−36.

(17) Misale, S.; Arena, S.; Lamba, S.; Siravegna, G.; Lallo, A.; Hobor, S.; Russo, M.; Buscarino, M.; Lazzari, L.; Sartorebianchi, A.; et al. Blockade of EGFR and MEK Intercepts Heterogeneous Mechanisms of Acquired Resistance to Anti-EGFR Therapies in Colorectal Cancer. *Sci. Transl. Med.* **2014**, *6* (224), 224ra26.

(18) Radstake, T. R. D. J.; van der Voort, R.; Brummelhuis, M. T.; de Waal Malefijt, M; Looman, M.; Figdor, C. G.; van den Berg, W.; Barrera, P.; Adema, G. J. Increased expression of CCL18, CCL19, and CCL17 by dendritic cells from patients with rheumatoid arthritis, and regulation by Fc gamma receptors. *Ann. Rheum. Dis.* **2004**, *64* (3), 359−367.

(19) Viola, A.; Contento, R. L.; Molon, B. T cells and their partners: The chemokine dating agency. *Trends Immunol.* **2006**, *27* (9), 421−427.

(20) Luster, A. D.; Bromley, S. K.; Mempel, T. R. Orchestrating the orchestrators: chemokines in control of T cell traffic. *Nat. Immunol.* **2008**, *9* (9), 970−980.

(21) Buonamici, S.; Trimarchi, T.; Ruocco, M. G.; Reavie, L.; Cathelin, S.; Mar, B. G.; Klinakis, A.; Lukyanov, Y.; Tseng, J. C.; Sen, F.; et al. CCR7 signalling as an essential regulator of CNS infiltration in T-cell leukaemia. *Nature* **2009**, *459* (7249), 1000−1004.

(22) Worbs, T.; Hammerschmidt, S. I.; Förster, R. Dendritic cell migration in health and disease. *Nat. Rev. Immunol.* **2017**, *17* (1), 30−48.

(23) Förster, R.; Davalosmisslitz, A. C.; Rot, A. CCR7 and its ligands: balancing immunity and tolerance. *Nat. Rev. Immunol.* **2008**, *8* (5), 362−371.

(24) Yin, H.; Kanasty, R. L.; Eltoukhy, A. A.; Vegas, A. J.; Dorkin, J. R.; Anderson, D. G. Non-viral vectors for gene-based therapy. *Nat. Rev. Genet.* **2014**, *15* (8), 541−555.

(25) Srinivasarao, M.; Galliford, C. V.; Low, P. S. Principles in the design of ligand-targeted cancer therapeutics and imaging agents. *Nat. Rev. Drug Discovery* **2015**, *14* (3), 203−219.

(26) Huang, S.; Duan, S.; Wang, J.; Bao, S.; Qiu, X.; Li, C.; Liu, Y.; Yan, L.; Zhang, Z.; Hu, Y. Folic Acid Mediated Functionalized Gold Nanocages for Targeted Delivery of Anti miR 181b in Combination of Gene Therapy and Photothermal Therapy against Hepatocellular Carcinoma. *Adv. Funct. Mater.* **2016**, *26* (15), 2532−2544.

(27) Müllerhermelink, N.; Braumüller, H.; Pichler, B.; Wieder, T.; Mailhammer, R.; Schaak, K.; Ghoreschi, K.; Yazdi, A.; Haubner, R.; Sander, C. A.; et al. TNFR1 Signaling and IFN-γ Signaling Determine whether T Cells Induce Tumor Dormancy or Promote Multistage Carcinogenesis. *Cancer Cell* **2008**, *13* (6), 507−518.

(28) Saito, T.; Nishikawa, H.; Nagano, Y.; Sugiyama, D.; Atarashi, K.; et al. Two FOXP3+CD4+ T cell subpopulations distinctly control the prognosis of colorectal cancers. *Nat. Med.* **2016**, *22* (6), 679−684.

(29) Gubin, M. M.; Zhang, X.; Schuster, H.; Caron, E.; Ward, J. P.; Noguchi, T.; Ivanova, Y.; Hundal, J.; Arthur, C. D.; Krebber, W. J. Checkpoint blockade cancer immunotherapy targets tumour-specific mutant antigens. *Nature* **2014**, *515* (7528), 577−581.

(30) Linnemann, C.; van Buuren, M. M.; Bies, L.; Verdegaal, E. M.; Schotte, R.; Calis, J. J.; Behjati, S.; Velds, A.; Hilkmann, H.; Atmioui, D. E.; et al. High-throughput epitope discovery reveals frequent recognition of neo-antigens by CD4+ T cells in human melanoma. *Nat. Med.* **2015**, *21* (1), 81−85.

(31) Hamanishi, J.; Mandai, M.; Matsumura, N.; Baba, T.; Yamaguchi, K.; Fujii, S.; Konishi, I. Activated local immunity by CC chemokine ligand 19-transduced embryonic endothelial progenitor cells suppresses metastasis of murine ovarian cancer. *Stem Cells* **2009**, *28* (1), 164−173.

(32) Roufaiel, M.; Gracey, E.; Siu, A.; Zhu, S. N.; Lau, A.; Ibrahim, H.; Althagafi, M.; Tai, K.; Hyduk, S. J.; Cybulsky, K. O.; et al. CCL19-CCR7-dependent reverse transendothelial migration of myeloid cells clears Chlamydia muridarum from the arterial intima. *Nat. Immunol.* **2016**, *17* (11), 1263−1272.

(33) Kiermaier, E.; Moussion, C.; Veldkamp, C. T.; Gerardy-Schahn, R.; De Vries, I.; Williams, L. G.; Chaffee, G. R.; Phillips, A. J.; Freiberger, F.; Imre, R.; et al. Polysialylation controls dendritic cell trafficking by regulating chemokine recognition. *Science* **2016**, *351* (6269), 186−190.

(34) Restifo, N. P.; Dudley, M. E.; Rosenberg, S. A. Adoptive immunotherapy for cancer: harnessing the T cell response. *Nat. Rev. Immunol.* **2012**, *12* (4), 269−281.

(35) Blattman, J. N.; Greenberg, P. D. Cancer immunotherapy: a treatment for the masses. *Science* **2004**, *305* (5681), 200−205.

(36) Figdor, C. G.; de Vries, I. J.; Lesterhuis, W. J.; Melief, C. J. Dendritic cell immunotherapy: mapping the way. *Nat. Med.* **2004**, *10* (5), 475−480.

(37) Moussion, C.; Girard, J. P. Dendritic cells control lymphocyte entry to lymph nodes through high endothelial venules. *Nature* **2011**, *479* (7374), 542−546.

(38) Kumar, V.; Donthireddy, L.; Marvel, D.; Condamine, T.; Wang, F.; Lavilla-Alonso, S.; Hashimoto, A.; Vonteddu, P.; Behera, R.; Goins, M. A. Cancer-Associated Fibroblasts Neutralize the Antitumor Effect of CSF1 Receptor Blockade by Inducing PMN-MDSC Infiltration of Tumors. *Cancer Cell* **2017**, *32* (5), 654−668.

(39) Thevenot, P.; Sierra, R.; Raber, P.; Al-Khami, A.; Trillo-Tinoco, J.; Zarreii, P.; Ochoa, A.; Cui, Y.; Delvalle, L.; Rodriguez, P. The Stress-Response Sensor Chop Regulates the Function and Accumulation of Myeloid-Derived Suppressor Cells in Tumors. *Immunity* **2014**, *41* (3), 389−401.

(40) Pollard, J. W. Tumour-educated macrophages promote tumour progression and metastasis. *Nat. Rev. Cancer* **2004**, *4* (1), 71−78.

(41) Murray, P. J.; Allen, J. E.; Fisher, E. A.; Gilroy, D. W.; Goerdt, S.; Gordon, S.; Hamilton, J. A.; Ivashkiv, L. B.; Lawrence, T. Macrophage activation and polarization: nomenclature and experimental guidelines. *Immunity* **2014**, *41* (1), 14−20.

(42) Mukhopadhyay, S.; Antalis, T. M.; Nguyen, K. P.; Hoofnagle, M. H.; Sarkar, R. Myeloid p53 regulates macrophage polarization and venous thrombus resolution by inflammatory vascular remodeling in mice. *Blood* **2017**, *129* (24), 3245−3255.

(43) Adachi, K.; Kano, Y.; Nagai, T.; Okuyama, N.; Sakoda, Y.; Tamada, K. IL-7 and CCL19 expression in CAR-T cells improves immune cell infiltration and CAR-T cell survival in the tumor. *Nat. Biotechnol.* **2018**, *36* (4), 346−351.